

Heavy metal removal by non-Newtonian emulsion liquid membrane dispersed in Taylor-Couette flow: experiments and modeling

Yong-Gyun Park^a, Dooil Kim^{b,*}

^aEnvironment Process Engineering Team, GS E&C, 33, Jong-ro, Jongno-gu, Seoul, 03159, Korea

^bDepartment of Civil & Environmental Engineering, Dankook University, 152, Jukjeon-ro, Suji-gu, Yongin-si, Gyeonggi-do, 16890, Korea, email: dikim21@dankook.ac.kr

Received 8 December 2015; Accepted 6 July 2016

ABSTRACT

The extraction of selected heavy metals from aqueous solutions was investigated using emulsion liquid membranes (ELMs). These ELMs were stabilized by converting the liquid (oil) membrane phase into non-Newtonian fluid through the addition of appropriate amounts of high-molecular-weight polymers. The resulting ELMs were further dispersed in Taylor-Couette flow to minimize emulsion breakage. In this ELM process, Cyanex 301, 302, and 923 and DEHPA were used as carrier agents to facilitate the transport of metals across the liquid (oil) membrane. A mathematical model to predict metal extraction was developed by taking into account the pH change in the external phase, the effect of agitation speed on the size of emulsion globules, and the leakage rate, based on a classical shrinking core model. The proposed mathematical model was found to have good agreement with the experimental results reasonably well and was shown to be useful to predict the performance of this particular ELM process under diverse operating conditions.

Keywords: Emulsion liquid membrane; Non-Newtonian conversion; Taylor-Couette flow; Heavy metals; Bis(2,4,4-trimethylpentyl)dithiophosphinic acid; Mathematical model

1. Introduction

Heavy metals, such as cadmium, lead, nickel, and zinc, are present in wastewaters produced from many metal processing industries, including metal mining, electroplating, extractive metallurgy, and metal treatment finishing, with typical concentrations ranging from 100 to 750 mg L⁻¹ [1–4]. Appropriate treatment of industrial wastewaters containing these heavy metals is important because of their serious impact on the natural environment as well as human health [2,5]. Common methods to remove heavy metals from wastewater include carbon adsorption, ion exchange, electro dialysis, electrolytic extraction, solvent extraction, and reverse osmosis [2]. However, these technologies suffer from various challenges such as high

construction and operating costs, considerable energy consumption, relatively low removal efficiency, operational complexity, and the requirement for additional purification processes [5,6].

Separation processes using emulsion liquid membranes (ELMs) have been studied because of the relatively low energy consumption, especially in comparison with processes such as electro dialysis and reverse osmosis [7], and the high extraction rate and efficiency due to the very large surface area available for mass transfer [8]. In particular, ELMs have been considered as a promising alternative technology for the removal and recovery of various heavy metals, such as cadmium, chromium, copper, nickel, and zinc [4,9–13], taking advantage of their high selectivity. This selectivity is achieved by using carrier agents in the membrane phase that exclusively bind target heavy metals and selectively shuttle them through the liquid membrane [8].

*Corresponding author.

Presented at the 8th International Conference on Challenges in Environmental Science & Engineering (CESE-2015), 28 September–2 October 2015, Sydney, Australia.

Nevertheless, the ELM process has not been much implemented in real industrial extraction processes because of its intrinsic problem, the instability of emulsion globules at a high fluid shear rate [14]. The ELM instability eventually causes the breakup of emulsion and the release of the internal stripping phase to the external phase, which nullify the overall solute extraction efficiency. Therefore, several solutions have been proposed to enhance the ELM stability including the addition of more surfactants and the usage of the viscous membrane solution. However, these solutions have some side effects. For example, surfactant at membrane interfaces can hinder the mass transfer [8] and cause the swelling problem of emulsion [15], and the viscous membrane solution can reduce the solute diffusivity [16–18]. Also, a polymeric porous membrane in a hollow fiber configuration was proposed, but it may have a fouling problem from the long time operation and a lower removal rate due to the relatively smaller surface area available for mass transfer [19–21].

Some solutions were proposed by our previous studies in order to enhance the stability of emulsion without scarifying the solute extraction efficiency of ELMs [22,23]. The first solution is to convert the membrane phase into a non-Newtonian form by dissolving small amount of high-molecular-weight polymers, polyisobutylene (PIB), which increase the viscosity of the membrane phase and the stability of emulsion without a decrease in diffusivity of solutes below the critical concentration of the polymer [16,24]. Additionally, smaller internal stripping phase droplets can be achieved to provide larger mass transfer area. The second solution was using a Taylor vortex column as a contacting reactor, which provides relatively uniform shear through the fluid, resulting in the minimization of the rupture of ELMs compared to conventional mixing reactors equipped with impellers [25]. And the Taylor vortex column requires less energy to disperse emulsions throughout the external feed phase [22,25].

The present study investigated the applicability of ELMs to the removal of common heavy metals, such as cadmium, lead, nickel, and zinc, from simulated industrial wastewater. It also examined the effects of membrane composition (e.g., type of carrier agent) and operating conditions (e.g., the external feed phase and the agitation speed of the Taylor vortex column) on the metal extraction rate. A mathematical model was developed to predict the removal rates of metal ions from unbuffered solutions by ELMs. In particular, the model incorporated the effects of changes in external phase pH, which were found to be important in determining the extraction efficiency of metal species with the carrier of choice.

2. Mathematical model description

The mathematical model presented here was developed based on a shrinking core model previously proposed by Liu for an ELM extracting a model amino acid [26]. Fig. 1 shows a schematic description of a single emulsion globule and the projected concentration profile of metal in the external feed phase and inside the emulsion globule. Because the Taylor vortex column provides relatively uniform and good mixing condition to the bulk phase at high agitation speed [22] and solute mass transfer through the film is not a large rate-limiting, the developed model assumed no concentration gra-

dient in the external phase. Furthermore, because the Biot number is usually larger than 20 under good mixing conditions, in which the decrease in emulsion globule size yields a high mass transfer surface area, the mass transfer coefficient in the external feed phase is significantly high, compared with that in the membrane phase [27]. The Biot number ($Bi = k_e R_{em} / m D_e$) represents the ratio of the mass transfer resistance inside the emulsion globules to that of the external feed phase [28,29], where k_e = mass transfer coefficient in the external phase film around the emulsion globule ($m s^{-1}$), R_{em} = radius of an emulsion globule (m), m = ratio of metal in the external feed phase to that in the membrane phase, and D_e = diffusivity of the metal-carrier complex in the membrane phase ($m^2 s^{-1}$). As carriers in the membrane phase complex with metal species at the interface of the emulsion and external phase, the complex first transports through the thin oil layer devoid of internal droplets [4,26]. As the metal-carrier complex moves further toward the center of the emulsion globule, the carrier quickly exchanges the bound metal with protons present in the internal phase. Because of the high viscosity of membrane phase and the presence of surfactants in the matrix of internal droplets, internal droplets are relatively motionless [4,30,31], and as a result, the protons in the internal droplets located away from the center of the globules are consumed first. As the exchange of metal and proton proceeds, a boundary forms inside the emulsion globule between the region containing 'exhausted' internal droplets and that containing 'unused' internal droplets (Fig. 1). This boundary, or reactive front, proceeds toward the center of the emulsion globule as the extraction progresses.

The mass balance of metal in the external phase can be expressed as:

$$\frac{dC_e}{dt} = -k_T a \cdot C_e + \Phi \cdot C_{em} \quad (1)$$

where C_e = the concentration of the metal in the external phase ($mol L^{-1}$), C_{em} = the concentration of the metal in the emulsion globule ($mol L^{-1}$), t = time (s), k_T = overall mass transport coefficient ($m s^{-1}$), a = specific surface area = $4 \cdot \pi \cdot r_e^2 \cdot N / V_e$ (m^{-1}), $k_T a$ = overall volumetric mass transfer coefficient (s^{-1}), r_e = radius of a single emulsion globule, N = total number of emulsion globules, V_e = volume of the external phase (m^3), and Φ = the leakage rate coefficient (s^{-1}). The first and second terms on the right side describe

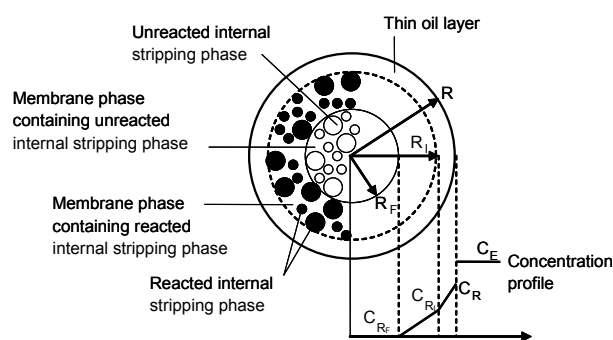


Fig. 1. Schematic of an emulsion globule and concentration profile. (R , R_e and R_F represent the radius of an emulsion globule, inner core, and reaction front, respectively.)

the extraction of the metal by the ELM and the release of metal due to ELM leakage, respectively. Though the size of individual emulsion globules might be affected by the swelling, coalescence, and redispersion of emulsions in this application, it was assumed in the model that emulsion globules were spheres of uniform size, and the average value measured was used for modeling.

From the overall mass balance of the metal:

$$C_{em} \cdot (V_m + V_i) = (C_{e0} - C_e) \cdot V_e \quad (2)$$

where C_{e0} = the initial concentration of the metal in the external feed phase (mol L^{-1}), V_m = volume of the membrane phase (m^3), and V_i = volume of the internal phase (m^3). Eq. (1) can be rewritten to eliminate C_{em} as:

$$\frac{dC_e}{dt} = -k_T a \cdot C_e + \Phi \cdot \frac{(C_{e0} - C_e) \cdot V_e}{V_m + V_i} \quad (3)$$

The overall mass transport coefficient, k_T , is further expressed as:

$$\frac{1}{k_T} = \frac{1}{k_e} + \frac{m}{k_{em}} \cong \frac{1}{k_{em}} = \left[\frac{(R_{em} - R_c)}{D_c} + \frac{(R_c - R_f)}{D_{em}} \right] \cdot m \quad (4)$$

where k_e = the mass transfer coefficient in the external phase film around the emulsion globule (m s^{-1}), k_{em} = the mass transfer coefficient in the emulsion globule (m s^{-1}), R_{em} = the radius of an emulsion globule (m), R_c = radius of the inner core of an emulsion globule (m), R_f = the radius of the reaction front (m), D_c = the diffusivity of the metal-carrier complex in the membrane phase ($\text{m}^2 \text{s}^{-1}$), D_{em} = the effective diffusivity of the metal-carrier complex in the emulsion ($\text{m}^2 \text{s}^{-1}$), and m = the ratio of the metal in the external feed phase to that in the membrane phase. At equilibrium, the estimated k_e is several hundred times larger than k_{em} , so the resistance ($1/k_e$) in the external feed phase is negligible.

Additional mass balance can be formulated by recognizing that metals extracted from the external phase primarily exist in a portion of the ELMs that contain exhausted internal droplets:

$$\frac{(C_{e0} - C_e)}{V_e} = \frac{4}{3} \pi \cdot (R_c^3 - R_f^3) \cdot \frac{V_i}{V_m + V_i} \cdot \left(\frac{R_{em}}{R_c} \right)^3 \cdot \alpha \cdot C_{s0} \cdot N \quad (0 \leq R_f \leq R_c) \quad (5)$$

where C_{s0} = the initial concentration of the internal stripping agent and α = the molar ratio of stripping agent reacting with the metal-carrier complex. Note that the $(R_{em}/R_c)^3$ term was used to account for the fact that a thin oil layer at the outer rim of the globule does not contain internal droplets. The set of Eqs. (3)–(5) was solved numerically through finite stepwise integration.

3. Experimental

3.1. Materials

Analytical-reagent-grade chemicals and water ($>20 \mu\Omega \text{ cm}^{-1}$ at 25°C) purified by a Milli-Q Ultrapure Gradient Water System (Millipore, Billerica, MA) were used throughout the study. Cyanex 301, 302, and 923 (Cytec Industries Inc., West Paterson, NJ) and DEHPA (Alfa Aesar, Ward Hill, MA) were used as carrier agents. Table 1 lists the relevant information about these compounds. The membrane phase consisted mainly of Soltrol 220 (Chevron Philips Chemical, Spring, TX). A non-ionic surfactant, Span 80, was used as an emulsifier, and PIB with an average molecular weight of 1,250,000 (ExxonMobil Chemical, Houston, TX) was used as the polymeric additive. The internal stripping phase was made of 2 M HNO_3 .

3.2. Experimental procedures

A Newtonian form of a solvent (Soltrol 220) was previously converted into a non-Newtonian form by PIB addition (5 g L^{-1}) to enhance the membrane's viscosity. Then, an emulsion was prepared by first dissolving Span 80 (5% w/v) and a carrier agent (0.1 M) into the membrane phase under gentle mixing with a magnetic stirrer. The prepared membrane phase was then placed in a 200-mL beaker immersed in an ice bath, and 25 mL of the internal stripping phase (2 M HNO_3) was added slowly under vigorous

Table 1
List of carrier agents employed in ELMs [42]

Carrier agents	Active components	Manufacturer or vendor	Formula	pK_a	Formula weight (g mol^{-1})
DEHPA	Di-(2-ethylhexyl)phosphoric acid	Alfa Aesar	$\text{C}_{16}\text{H}_{35}\text{O}_4\text{P}$		322.40
Cyanex 301	Bis(2,4,4-trimethylpentyl)dithiophosphinic acid	Cytec	$\text{C}_{16}\text{H}_{35}\text{PS}_2$	2.61*	322.55
Cyanex 302	Bis(2,4,4-trimethylpentyl) monothiophosphinic acid	Cytec	$\text{C}_{16}\text{H}_{35}\text{PSO}$	5.63*	306.49
Cyanex 923	Trihexylphosphine oxide Dihexylmonoocetylphosphine oxide Diocetylmonohexylphosphine oxide Triocetylphosphine oxide	Cytec	$\text{C}_{18}\text{H}_{39}\text{OP}$		302.48

* At 24°C

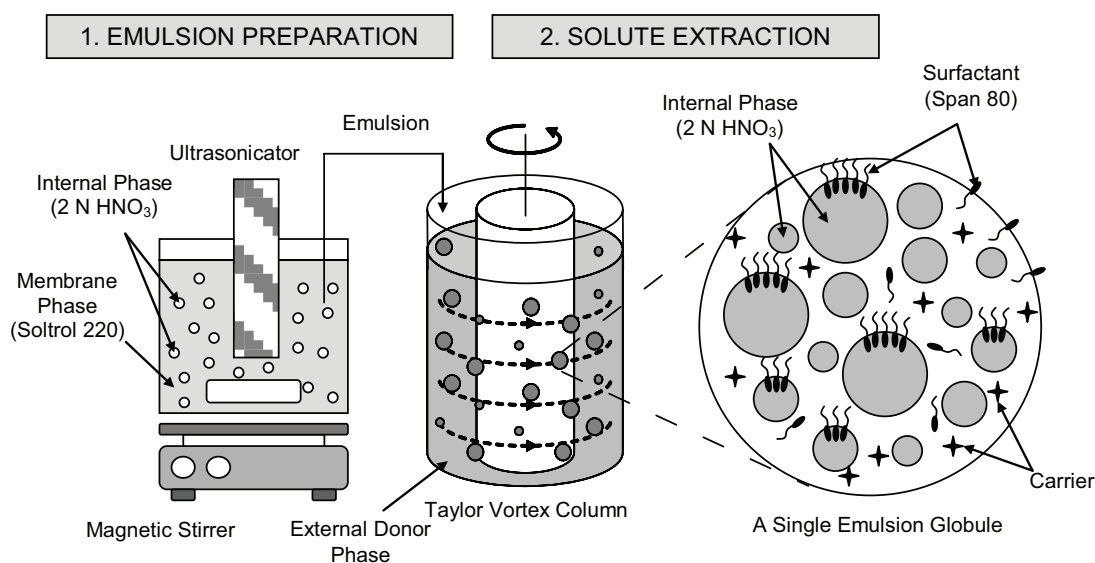


Fig. 2. Schematic of experimental apparatus [23].

mixing with sonication. This process is described in detail in Park et al. [22].

Solute extraction was performed using a custom-built Taylor vortex column, shown in Fig. 2. The column consisted of an inner cylinder made of polytetrafluoroethylene with a diameter of 49.3 mm and a height of 94.0 mm, and an outer cylinder made of glass with an inner diameter of 80.5 mm and a height of 100.9 mm. The inner cylinder was housed within the fixed outer cylinder and connected to a variable speed motor. An aqueous donor phase (the model industrial wastewater) of 200 mL containing heavy metals (0.01 M or 0.0025 M) was kept in the annular gap between the inner cylinder and the outer cylinder. While rotating the inner cylinder at a rotational velocity of 400–600 rpm (6900–10,000 Taylor number), 20 mL of prepared emulsion was injected into the middle of the donor phase by pipette to initiate the extraction process. The temperature was controlled at 20°C.

3.3. Sample collection and analysis

Samples (3 mL) were collected periodically from the agitated solution located at the middle of the Taylor vortex column using a micropipette. Collected samples were immediately filtered using a polypropylene syringe filter with nominal pore size of 0.2 μm (Pall Co., East Hills, NY). Concentrations of heavy metals studied were analyzed by inductively coupled plasma mass spectrometer-atomic emission spectroscopy (ICP-AES) (Model ICAP 61E Trace Analyzer, Thermo Jarrell Ash, Franklin, MA). The detection wavelengths for cadmium, lead, nickel, and zinc were 226.502, 220.353, 231.604, and 206.200 nm, respectively. Nitric acid (1%) was used as a rinse solution. For instrument calibration, standard solutions of each species were prepared with high-purity standards (Charleston, SC) and Milli-Q water. Analyses were performed four times for each sample, and average values were recorded.

Nitrate concentrations in samples collected from emulsion leakage experiments were measured using a Dionex DX-600 ion chromatography (IC) system (Sunnyvale, CA),

consisting of a GP50 gradient pump, IonPac AG9-HC guard column, IonPac AS9-HC analytical column (4 × 250 mm), Anionic Atlas Electrolytic suppressor (AAES), and ED50 conductivity detector. The collected samples were injected with an AS50 autosampler. Sodium carbonate (Na₂CO₃; 9.0 mM) was used as the eluent at a flow rate of 1.3 mL min⁻¹. The applied current was 100 mA, and the elution time of nitrate was 9.5 min.

4. Results and discussion

4.1. Effect of carrier type and pH

Initial experiments were performed to extract zinc from the aqueous phase using ELMs containing three different carrier agents: Cyanex 301, Cyanex 302, and Cyanex 923. These are available commercially and used commonly for the selective removal of metal ions in solvent and liquid membrane extraction processes [32–37]. Experiments were performed individually under the same conditions: $C_{z0} = 0.01$ M zinc, $C_{s0} = 2$ M HNO₃, $C_c = 0.1$ M (different carriers), concentration of Span 80 = 5% w/v, concentration of PIB = 5 g L⁻¹, $V_i/V_m = 0.33$, $V_o/V_f = 0.1$, agitation speed = 500 rpm, and temperature = 20°C. The experimental results (Fig. 3) suggested that Cyanex 923 was not effective for zinc removal. While Cyanex 923 bound strongly to zinc and thus might be useful in solvent extraction [38,39], its exceedingly high affinity for zinc did not allow later separation during stripping [40]. Inefficient stripping in the internal phase makes this chemical unsuitable as a carrier in the ELM extraction process. Cyanex 302, which has one thiol group, was found to be less effective than Cyanex 301, which has two thiol groups.

The observed differences in extraction efficiency between the carriers became more evident when the external pH was varied. Experiments were performed using Cyanex 301 and 302 as carrier agents with the external phase pH adjusted with nitric acid addition (the adjusted pHs by adding 0, 0.1, 0.5, and 1 M of HNO₃ were initially 5.17, 1.63, 0.54, and 0.35,

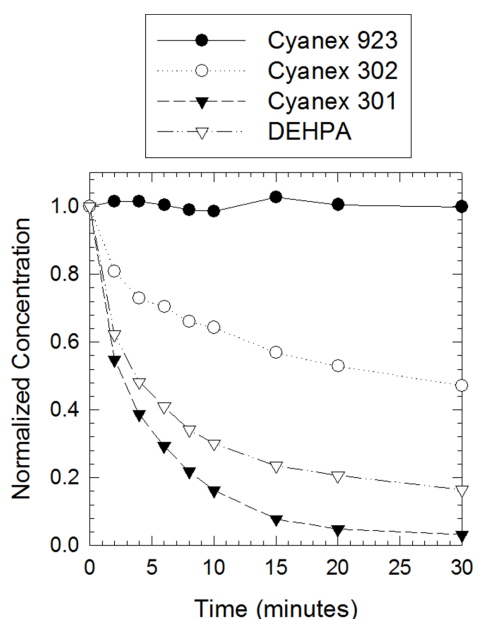


Fig. 3. Zinc extraction with various types of carrier agents ($C_{e0} = 0.01$ M; $C_c = 0.1$ M, each; $C_{s0} = 2$ M HNO_3 ; Span 80 concentration = 5% w/v; PIB concentration = 5 g L^{-1} ; $V_i/V_m = 0.33$; $V_e/V_f = 0.1$; agitation speed = 500 rpm; and temperature = 20°C).

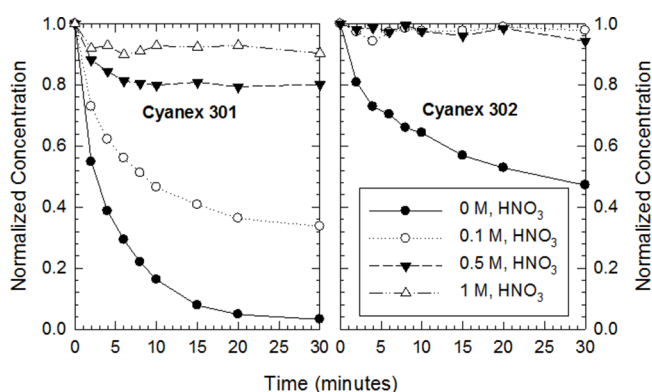


Fig. 4. Effect of the pH of the external feed phase adjusted by nitric acid addition on zinc extraction ($C_{e0} = 0.01$ M; $C_c = 0.1$ M, Cyanex 301 or 302; $C_{s0} = 2$ M HNO_3 ; Span 80 concentration = 5% w/v; PIB concentration = 5 g L^{-1} ; $V_i/V_m = 0.33$; $V_e/V_f = 0.1$; agitation speed = 500 rpm; and temperature = 20°C).

respectively). The experimental results (Fig. 4) suggested that zinc removal with Cyanex 302 was more strongly affected by pH decrease than that with Cyanex 301 in the pH range tested. This might have been the result of Cyanex 302 having a higher acid-base dissociation constant, $\text{p}K_a$ of 5.63, than Cyanex 301 ($\text{p}K_a = 2.61$) [41], such that more thiol groups in Cyanex 302 were protonated and became less efficient in binding metals. Note that protons are exchanged during the extraction and the pH decreases continuously during the extraction process [12,41,42]. Additionally, the leakage of emulsion globules adds a stripping agent (HNO_3) to the external phase, which further contributes to the pH decrease. Thus, the rate (slope) of metal extraction in Figs. 3 and 4 decreases continuously

(i.e., the curves were concave upward) not only due to the decrease in the concentration difference between the external and internal phases as the extraction proceeded (i.e., decrease in driving force), but also the decrease in the external phase pH, resulting from proton exchange and ELM leakage. The model presented in the previous section was therefore developed to account for the pH-dependent equilibrium of metal and carrier complexation. The next section describes the results of the model tested using Cyanex 301, apparently the most suitable carrier agent for the chosen system.

4.2. Model parameter evaluation

Key model parameters were estimated empirically or theoretically. The average radii of emulsion globules (R_{em}) and internal droplets (R_i) were measured directly by a photographic method. The average radius of emulsion globules was determined to be 1.5×10^{-4} m at an inner cylinder rotation speed of 500 rpm by first photographing with a digital camera and subsequent digital magnification and analysis of more than 200 individual globule images. The measurement of dispersed internal droplet size was performed within 10 min after preparing the W/O emulsions ($C_c = 0.1$ M, Cyanex 301, $C_{s0} = 2$ M HNO_3 , Span 80 concentration = 5% w/v, PIB concentration = 5 g L^{-1} , and $V_i/V_m = 0.33$). The prepared emulsion samples (< 0.5 mL) were placed on a glass slide. Then, each sample was covered with a thin cover glass, and the photomicrographs were taken using a Leica DM IRM differential interference contrast (DIC) microscope (Wetzlar, Germany) operated in a reflective index mode and a Hamamatsu EM-CCD C9100 CCD camera (1000 × 1000 pixels, 0.53 μm resolution/pixel, Hamamatsu City, Japan). In reflected light DIC microscopy, the discontinuity on the surface of water in oil creates an optical path difference, which reveals the topographical profile. This microscopic technique provided relatively clean images of individual internal droplets. The average radius of the internal droplets was estimated to be 1.0×10^{-6} m.

From these experimentally determined R_{em} and R_i values, the thickness of the thin oil layer ($R_{em} - R_c$) and hence the radius of the initial reaction front (R_c) were estimated at 9.5×10^{-7} and 1.4530×10^{-4} m, respectively, according to the following equation:

$$R_{em} - R_c = \left(\frac{4\pi}{3}\right)^{1/3} R_i \left[\left(\frac{V_i}{V_m + V_i}\right)^{-1/3} - 1 \right] \quad (6)$$

The diffusivity of the metal-carrier complex in the membrane phase (the thin oil layer) was estimated to be 7.5783×10^{-11} ($\text{m}^2 \text{s}^{-1}$) using the Hayduk and Minhas correlation [43]:

$$D_c (\text{m}^2 / \text{s}) = 13.3 \times 10^{-8} \frac{T^{1.47} \mu_m^c}{V_c^{0.71}} \quad (7)$$

where T = absolute temperature (K), μ_m = the viscosity of the membrane (cP), and V_c = the molar volume of the complex at its normal boiling point ($\text{cm}^3 \text{mol}^{-1}$), which was estimated to be $881.6 \text{ cm}^3 \text{mol}^{-1}$, according to the Le Bas method [43], assuming that the molar volume of the tested metals was negligible. A value of 10.7 cP was used for the membrane viscosity (μ_m) [16].

The effective diffusivity of the metal-carrier complex in the emulsion was estimated to be $3.9442 \times 10^{11} \text{ m}^2 \text{ s}^{-1}$, by the following Jefferson-Witzell-Sibbitt correlation [4]:

$$D_{em} (\text{m}^2 / \text{s}) = 10^4 D_c \left[\frac{4(1+2p)^2 - \pi}{4(1+2p)^2} \right] \quad (8)$$

$$\text{where } p = 0.103 \left(\frac{V_i}{V_m + V_i} \right)^{-1/3} - 0.5.$$

A separate set of batch extraction experiments was performed to evaluate the stoichiometry of the metal-carrier reaction (Fig. 5). An aqueous solution (200 mL) containing four different metals (individually) at an initial concentration of 0.01 M was contacted with a membrane phase (Soltrol 220, 15 mL) containing 0.1 M of Cyanex 301. The membrane phase also contained 5 g L^{-1} of PIB but no surfactant. Gentle mixing was conducted with a magnetic stirrer at 20°C , and changes in the concentration of the aqueous donor phase were monitored. After reaching equilibrium and from the concentrations of metal remaining in the aqueous phase, the mole ratios of Cyanex 301 to cadmium, lead, nickel, and zinc were determined as 2.16, 2.02, 2.19, and 2.32, respectively. From these results, the following equilibrium reaction with the correct stoichiometry can be expressed as:



where M^{2+} = metal in the external phase, \overline{HL} = carrier in the membrane phase (bound to protons), and \overline{ML}_2 = metal-carrier complex in the membrane phase. Note that because the carrier is present in protonated form in the membrane phase, one mole of carriers releases two moles of protons, and therefore, in Eq. (5), $\alpha = 2$. From this equilibrium relationship, the distribution coefficient, m , in Eq. (4) can be further defined as:

$$m = \frac{C_{M^{2+}}}{C_{\overline{ML}_2}} = \frac{C_{H^+}^2}{K_{ex} \cdot C_{HL}} \quad (10)$$

where $C_{M^{2+}}$ = the concentration of the metal in the external phase (mol L^{-1}), $C_{\overline{ML}_2}$ = the concentration of the metal-carrier

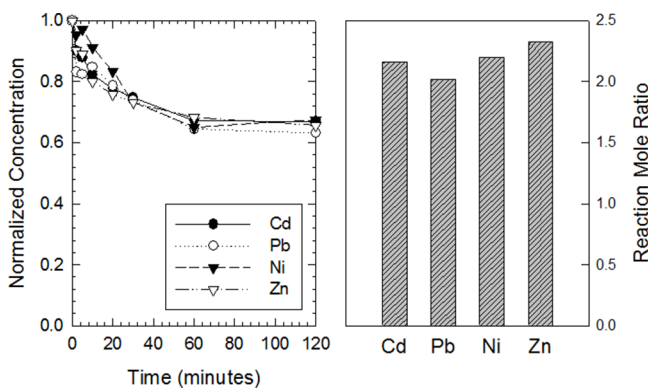


Fig. 5. Metal extraction by a shaker test with Cyanex 301: a. metal concentration decrease during a shaker test and b. complexation mole ratio of Cyanex 301 with cadmium, lead, nickel, and zinc ($C_{e0} = 0.01 \text{ M}$; $C_c = 0.1 \text{ M}$, Cyanex 301; PIB concentration = 5 g L^{-1} ; $V_m/V_c = 0.075$; and temperature = 20°C).

complex in the membrane phase (mol L^{-1}), C_{H^+} = the concentration of protons in the external phase (mol L^{-1}), C_{H^+} = the concentration of carrier in the membrane phase (mol L^{-1}), and K_{ex} = the equilibrium constant for metal-carrier complex formation (i.e., equilibrium constant for reaction [9]). In an excess carrier to metal condition, $C_{HL} \gg C_{\overline{ML}_2}$, and $C_{HL} \cong C_{HL,0}$, the initial carrier concentration in the membrane phase.

Another set of experiments was performed to determine the leakage rate coefficient (Φ). The concentration of nitrate in the external phase originating from the internal phase during ELM breakage was measured as a function of time. Because the pH of the external feed phase during the metal extraction in this study typically ranged from 2.5 to 1.6, four different acidic buffer solutions (0.36 M HCl, 0.12 M HCl, 0.2 M H_3PO_4 , and 0.2 M CH_3COOH ; pH = 1.13, 1.44, 1.71, and 2.65, respectively) were used as the external feed phase. In this study, only acid components were used to provide specific initial pHs of the external feed phase because metal ions can make a complex with basic components, resulting in precipitation. The relatively high buffering capacity of the solutions examined minimized changes in pH of the external feed phase during metal extraction that resulted from hydrogen ion release by the leakage of emulsion and by extraction and stripping reactions driven by the carrier. Fig. 6 presents the experimental results. The rate of leakage was constant over more than 30 min (i.e., linear slope), with the rate varying

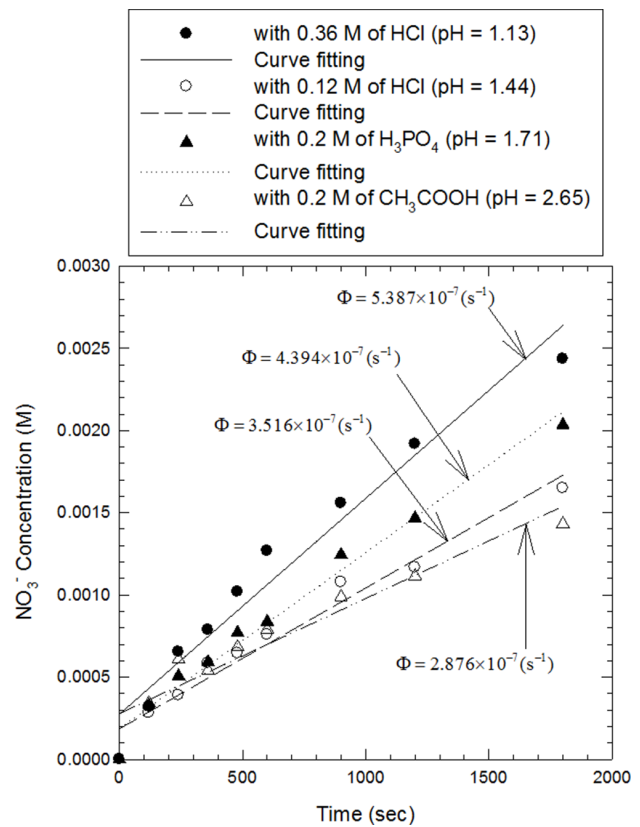


Fig. 6. Leakage experiment results for various types of the external feed phase ($C_c = 0.1 \text{ M}$, Cyanex 301; $C_{s0} = 2 \text{ M HNO}_3$; Span 80 concentration = 5% w/v; PIB concentration = 5 g L^{-1} ; $V_m/V_c = 0.33$; $V_d/V_f = 0.1$; agitation speed = 500 rpm; and temperature = 20°C).

from 2.876×10^{-7} to $5.387 \times 10^{-7} \text{ s}^{-1}$. The average leakage rate coefficient ($4.156 \times 10^{-7} \text{ s}^{-1}$) was used in the mathematical modeling prediction of the metal removal rate.

Modeling prediction still involved two key unknown parameters: changes in hydrogen ion concentration in the external feed phase (i.e., decreased pH) throughout the ELM process and the equilibrium reaction constant, K_{ex} . For the former, a separate experiment was conducted to determine the profile of the changes in pH during the external feed phase. The following equation expresses the proton concentration in the external phase, derived from pH measurements during metal extraction:

$$[H^+] = 0.00813 + 0.00481 \cdot (1 - \exp(-0.07323 \times t)) \quad (11)$$

where $[H^+]$ = the concentration of protons in the external phase (mol L^{-1}) and t = contact time (min). This equation appropriately indicated the changes in pH in the external phase during metal extraction, although the initial proton concentration was not estimated precisely due to the sudden increase in pH caused by the emulsion injection to initiate the metal extraction.

4.3. Model verification

Fig. 7 shows the extraction of four different heavy metals by the ELM process, determined experimentally versus that predicted with the proposed model. Note that the

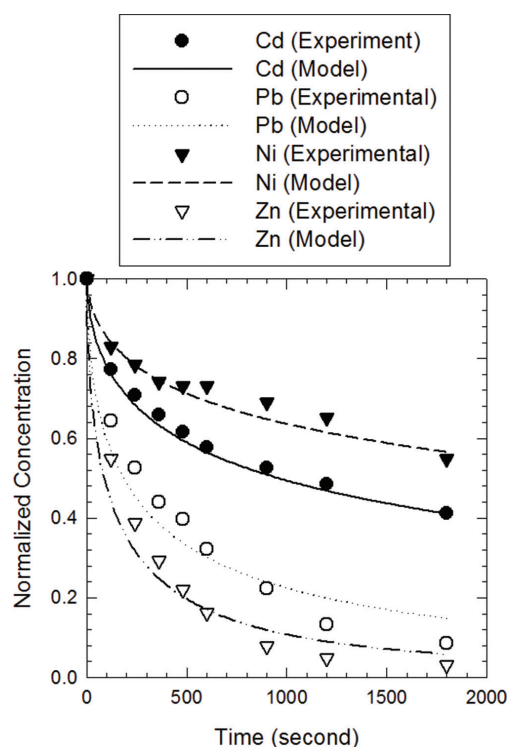


Fig. 7. Comparison of the modeling prediction with the experimental results of the extraction rates of cadmium, lead, nickel, and zinc ($C_{e0} = 0.01 \text{ M}$; $C_c = 0.1 \text{ M}$, Cyanex 301; $C_{s0} = 2 \text{ M HNO}_3$; Span 80 concentration = 5% w/v; PIB concentration = 5 g L^{-1} ; $V_i/V_m = 0.33$; $V_j/V_f = 0.1$; agitation speed = 500 rpm; and temperature = 20°C).

equilibrium constant K_{ex} is still unknown. To estimate K_{ex} , the concentration of a solute-carrier complex in the liquid membrane phase needs to be measured; however, this is not a simple matter for a particular ELM system. Thus, the equilibrium constants for zinc, lead, cadmium, and complexation with Cyanex 301 obtained by a least-square approach based on metal concentrations were 0.0034, 0.0018, 0.0005, and 0.00023, respectively. The model curves matched the experimental results very well.

Fig. 8 shows the experimental data for zinc extraction under varying rotation speeds of the inner cylinder in the Taylor vortex column. These rotation speeds correspond to a dimensionless Taylor number, Ta , of approximately 6900–10,000. Ta is defined as follows:

$$Ta = \frac{2\pi R' S d_g}{\nu} \sqrt{\frac{d_g}{R'}} \quad (12)$$

where R' = the radius of the rotor (m), S = the rotational speed (rps), d_g = the annular gap width (m), and ν = the kinematic viscosity ($\text{m}^2 \text{ s}^{-1}$) of the external feed phase at 20°C in an ELM system [44]. As the rotation speed increases, the size of the emulsion globules becomes smaller (consequently, the total available reaction surface area increases), and the rate of leakage increases, both due to increased fluid shear. The radii of the emulsion globules at 400 and 600 rpm were measured as 1.8×10^{-4} and $1.0 \times 10^{-4} \text{ m}$, respectively, following the same procedure that was used at 500 rpm. The leakage

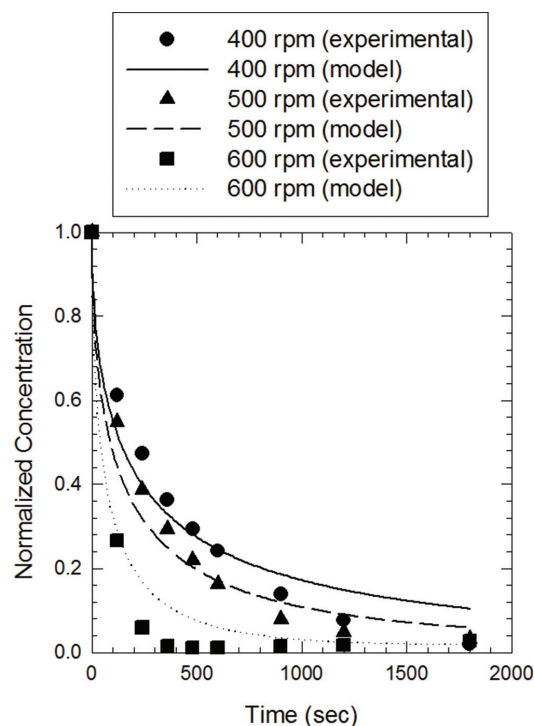


Fig. 8. Comparison of the model prediction with the experimental results for the effect of agitation speed on metal extraction ($C_{e0} = 0.01 \text{ M}$, zinc; $C_c = 0.1 \text{ M}$, Cyanex 301; $C_{s0} = 2 \text{ M HNO}_3$; Span 80 concentration = 5% w/v; PIB concentration = 5 g L^{-1} ; $V_i/V_m = 0.33$; $V_j/V_f = 0.1$; agitation speed = 400, 500, and 600 rpm; and temperature = 20°C).

rates at 400 and 600 rpm were estimated as 3.138×10^{-7} and $5.108 \times 10^{-7} \text{ s}^{-1}$, respectively, according to a correlation, $\Phi \propto S^{1.2}$, where S = the rotation speed of the inner cylinder [22]. Other model parameters remained constant. The model predictions in Fig. 8 matched the experimental data reasonably well. Some underprediction in extraction rates was observed at higher rotation speeds, presumably due to inaccuracy in photographic size measurements of the emulsion globules at higher speeds as they became smaller.

Experiments in this section were performed to evaluate the efficiency of ELMs with Cyanex 301 ($C_c = 0.1 \text{ M}$) in treating a mixture solution containing cadmium, lead, nickel, and zinc ($C_{e0} = 2.5 \text{ mM}$, each metal). Fig. 9 presents the results obtained through the experiments. The order of the removal rate of the metals tested was $\text{Pb} > \text{Cd} \gg \text{Zn} > \text{Ni}$. The removal rates of zinc and nickel were found to be greatly influenced when they treated with the other competing metal ions, such as lead and cadmium (compared with the results shown in Fig. 7). This can be explained by the selectivity (affinity) of the carrier for the metal [45]. Thus, it is assumed that in the modeling predictions, the selective transport of metals by ELMs were related mainly to the amount of available carrier applied. By manipulating the carrier concentration (i.e., the actual concentration of carriers available, $C_c' = \beta \cdot C_c$, where β = an empirical constant) in the model, the removal rate of each metal from the mixture solution was estimated and then compared with the experimental data (Fig. 9). The empirical constants used in the modeling prediction for cadmium, lead, nickel, and zinc were 1, 1, 0.1, and 0.055, respectively. The model predictions underestimated the removal rate of cadmium by ELMs with Cyanex 301.

4.4. Model application

The model developed in this study could be a useful tool to predict the performance of the ELM process in diverse operating conditions. Fig. 10 presents an example model application, showing zinc extraction efficiency, expressed in terms of the removal ratio after 10 min of contact time,

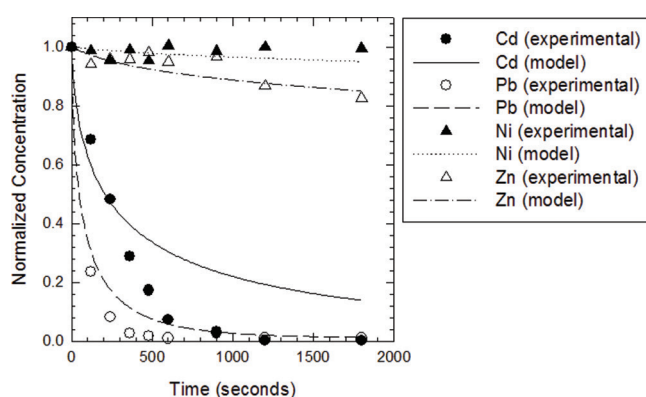


Fig. 9. Comparison of model prediction with experimental results of multi-metal removal by emulsion liquid membranes (ELMs) ($C_{e0} = 0.0025 \text{ M}$, each; $C_c = 0.1 \text{ M}$, Cyanex 301; $C_{s0} = 2 \text{ M HNO}_3$; Span 80 concentration = 5% w/v; PIB concentration = 5 g L^{-1} ; $V_c/V_m = 0.33$; $V_c/V_f = 0.1$; agitation speed = 500 rpm; and temperature = 20°C).

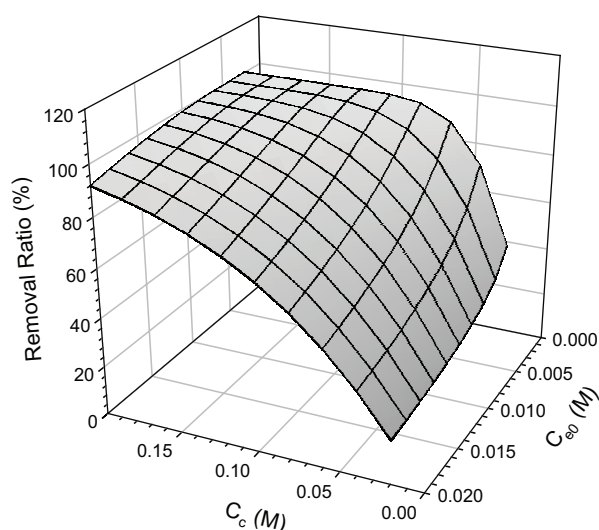


Fig. 10. Modeling prediction of zinc removal ratio (%) by ELMs with Cyanex 301 at 10 min of contact time.

under varying zinc and Cyanex 301 concentrations at 500 rpm. The dosage of the carrier agent in proportion to the concentration of the target metal is one important operating parameter to be considered in real applications. The other model parameters were the same as used in the section above. The applied initial concentrations of zinc and Cyanex 301 were 0.002–0.02 M and 0.02–0.200 M, respectively. It was predicted that as the applied carrier concentration increased at a fixed metal concentration, or as metal concentration decreased at a fixed carrier concentration, the ELM removal efficiency for the zinc solution would be enhanced. To achieve more than 90% removal of metals in this example ELM system, this graph suggests that the carrier concentration should be adjusted from 0.06 M (for 0.002 M of zinc) to 0.2 M (for 0.02 M of zinc). That is, when treating higher concentrations of zinc, higher concentrations of carrier are required to achieve a certain level of ELM removal efficiency. Additionally, the zinc removal ratio by ELMs was enhanced at longer contact times. For example, under conditions of 0.002 M of initial zinc concentration and 0.06 M of carrier concentration, the estimated zinc removal ratios were 91.9% and 98.2% (data not shown) at 10 and 30 min of contact time, respectively.

5. Conclusions

This non-Newtonian ELM dispersed in Taylor-Couette flow was shown to be a very promising technology for extracting a relatively large amount of heavy metal (10 mM) from model industrial wastewaters. Among the carriers tested, Cyanex 301 was the most suitable. The pH dependency of the extraction was taken into consideration to develop a modified version of a shrinking core model that predicts the extraction rate of metal by ELMs. Model predictions matched the experimental data reasonably well, while fitting the unknown equilibrium constant remains a major drawback of the proposed model. Nonetheless, the model should provide a useful

tool for predicting the performance of the metal extraction process by this particular ELM system, as shown in the sample application, estimating metal extraction efficiencies under varying metal and carrier concentrations.

Acknowledgments

The present research was supported by the research fund from Dankook University in 2014. The authors thank Dr. K.C. Pathak for his contribution during the earlier phase of this project and Dr. Guangxuan Zhu for assistance in maintenance and troubleshooting of ICP-AES.

References

- [1] A.J.B. Dutra, A. Espinola, P.P. Borges, Cadmium removal from diluted aqueous solutions by electrowinning in a flow-by cell, *Miner. Eng.*, 13 (2000) 1139–1148.
- [2] M. Loaec, R. Olier, J. Guezennec, Uptake of lead, cadmium and zinc by a novel bacterial exopolysaccharide, *Water Res.*, 31 (1997) 1171–1179.
- [3] M.J. Schwuger, G. Subklew, N. Woller, New alternatives for waste water remediation with complexing surfactants, *Colloids Surf., A: Physicochem. Eng. Asp.*, 186 (2001) 229–242.
- [4] M. Chakraborty, C. Bhattacharya, S. Datta, Study of the stability of W/O/W-type emulsion during the extraction of nickel via emulsion liquid membrane, *Sep. Sci. Technol.*, 39 (2004) 2609–2625.
- [5] A. Zouboulis, C.A. Prochaska, P.M. Solozhenkin, Removal of zinc from dilute aqueous solutions by galvanochemical treatment, *J. Chem. Technol. Biotechnol.*, 80 (2005) 553–564.
- [6] A.H.M. Veeken, L. Akoto, L.W. Hulshoff Pol, J. Weijma, Control of the sulfide (S^{2-}) concentration for optimal zinc removal by sulfide precipitation in a continuously stirred tank reactor, *Water Res.*, 37 (2003) 3709–3717.
- [7] M.M. Naim, A.A. Monir, Desalination using supported liquid membranes, *Desalination*, 153 (2003) 361–369.
- [8] J.W. Frankenfeld, N.N. Li, *Recent Advances in Liquid Membrane Technology*, Handbook of Separation Process Technology, Wiley, New York, 1987.
- [9] R.M. Izatt, R.L. Bruening, G.A. Clark, J.D. Lamb, J.J. Christensen, Effect of macrocycle type on Pb^{2+} transport through an emulsion liquid membrane, *Sep. Sci. Technol.*, 22 (1985) 661–675.
- [10] R.P. Schwarzenbach, P.M. Gschwend, D.M. Imboden, *Environmental organic chemistry*, J. Wiley, New York 2003.
- [11] B.J. Raghuraman, N.P. Tirmizi, B.S. Kim, J.M. Wiencek, Emulsion liquid membranes for wastewater treatment. Equilibrium models for lead- and cadmium-di-2-ethylhexyl phosphoric acid systems, *Environ. Sci. Technol.*, 29 (1995) 979–984.
- [12] M.T.A. Reis, J.M.R. Carvalho, Recovery of zinc from an industrial effluent by emulsion liquid membranes, *J. Membr. Sci.*, 84 (1993) 201–211.
- [13] F. Valenzuela, J. Cabrera, C. Basualto, J. Sapag-Hagar, Kinetics of copper removal from acidic mine drainage by a liquid emulsion membrane, *Miner. Eng.*, 18 (2005) 1224–1232.
- [14] A. Ahmad, A. Kusumastuti, M.S. Buddin, C. Derek, B. Ooi, Emulsion liquid membrane based on a new flow pattern in a counter rotating Taylor-Couette column for cadmium extraction, *Sep. Purif. Technol.*, 127 (2014) 46–52.
- [15] T. Kinugasa, K. Watanabe, H. Takeuchi, Effect of organic solvents on stability of liquid surfactant membranes, *J. Chem. Eng. Jpn.*, 22 (1989) 593–597.
- [16] A.H.P. Skelland, X. Meng, New solution to emulsion liquid membrane problems by non-Newtonian conversion, *AIChE J.*, 42 (1996) 547–561.
- [17] R.E. Terry, N.N. Li, W.S. Ho, Extraction of phenolic compounds and organic acids by liquid membranes, *J. Membr. Sci.*, 10 (1982) 305–323.
- [18] W. Hou, K.D. Papadopoulos, W1/O/W2 and O1/W/O2 globules stabilized with span 80 and tween 80, *Colloids Surf., A: Physicochemical and Engineering Aspects*, 125 (1997) 181–187.
- [19] A. Nanoti, S.K. Ganguly, A.N. Goswami, B.S. Rawat, Removal of phenols from wastewater using liquid membranes in a microporous hollow-fiber-membrane extractor, *Ind. Eng. Chem. Res.*, 36 (1997) 4369–4373.
- [20] G.R.M. Breembroek, A. van Straalen, G.J. Witkamp, G.M. van Rosmalen, Extraction of cadmium and copper using hollow fiber supported liquid membranes, *J. Membr. Sci.*, 146 (1998) 185–195.
- [21] S.Y.B. Hu, J.M. Wiencek, Emulsion-liquid-membrane extraction of copper using a hollow-fiber contactor, *AIChE J.*, 44 (1998) 570–581.
- [22] Y. Park, L.J. Forney, J.H. Kim, A.H.P. Skelland, Optimum emulsion liquid membranes stabilized by non-Newtonian conversion in Taylor-Couette flow, *Chem. Eng. Sci.*, 59 (2004) 5725–5734.
- [23] Y. Park, A.H.P. Skelland, L.J. Forney, J.H. Kim, Removal of phenol and substituted phenols by newly developed emulsion liquid membrane process, *Water Res.*, 40 (2006) 1763–1772.
- [24] A.H.P. Skelland, X. Meng, Non-Newtonian conversion solves problems of stability, permeability, and swelling in emulsion liquid membranes, *J. Membr. Sci.*, 158 (1999) 1–15.
- [25] L.J. Forney, A.H.P. Skelland, J.F. Morris, R.A. Holl, Taylor vortex column: Large shear for liquid-liquid extraction, *Sep. Sci. Technol.*, 37 (2002) 2967–2986.
- [26] X. Liu, D. Liu, A mass transfer resistance analysis of L-tryptophan extraction in an emulsion liquid membrane system, *Sep. Sci. Technol.*, 35 (2000) 2707–2724.
- [27] W.S.W. Ho, K.K. Sirkar, *Membrane handbook*, Chapman & Hall, New York, 1992.
- [28] A.N. Goswami, T.C.S.M. Gupta, S.K. Sharma, A. Sharma, R. Krishna, Unsteady-state modeling and analysis for liquid surfactant membrane hydrocarbon separation processes, *Ind. Eng. Chem. Res.*, 32 (1993) 634–640.
- [29] N. Yan, Y. Shi, Y.F. Su, Mass transfer model for type i facilitated transport in liquid membranes, *Chem. Eng. Sci.*, 47 (1992) 4365–4371.
- [30] R.P. Borwankar, C.C. Chan, D.T. Wasan, R.M. Kurzeja, Z.M. Gu, N.N. Li, Analysis of the effect of internal phase leakage on liquid membrane separations, *AIChE J.*, 34 (1988) 753–762.
- [31] R. Chowdhury, P. Bhattacharya, Mathematical analysis of unsteady-state dynamics of a liquid-membrane-encapsulated urease system, *Ind. Eng. Chem. Res.*, 36 (1997) 5467–5473.
- [32] B. Gupta, A. Deep, V. Singh, S.N. Tandon, Recovery of cobalt, nickel, and copper from sea nodules by their extraction with alkylphosphines, *Hydrometallurgy*, 70 (2003) 121–129.
- [33] L.J. Lozano, C. Godinez, F.J. Alguacil, Facilitated transport of vanadium (V) by supported liquid membranes, *Hydrometallurgy*, 80 (2005) 196–202.
- [34] A.M. Rodriguez, D. Gomez-Limon, F.J. Alguacil, Liquid-liquid extraction of cadmium(II) by Cyanex 923 and its application to a solid-supported liquid membrane system, *J. of Chem. Technol. Biotechnol.*, 80 (2005) 967–972.
- [35] I. Van de Voorde, L. Pinoy, R.F. De Ketelaere, Recovery of nickel ions by supported liquid membrane (SLM) extraction, *J. Membr. Sci.*, 234 (2004) 11–21.
- [36] Y.K.P. Sze, L. Xue, Extraction of zinc and chromium(III) and its application to treatment of alloy electroplating wastewater, *Sep. Sci. Technol.*, 38 (2003) 405–425.
- [37] C. Koopman, G.J. Witkamp, G.M. Van Rosmalen, Removal of heavy metals and lanthanides from industrial phosphoric acid process liquors, *Sep. Sci. Technol.*, 34 (1999) 2997–3008.
- [38] R. Cierpiszewski, I. Miesiac, M. Regel-Rosocka, A.M. Sastre, J. Szymanowski, Removal of zinc(II) from spent hydrochloric acid solutions from zinc hot galvanizing plants, *Ind. Eng. Chem. Res.*, 41 (2002) 598–603.
- [39] M. Regel, A.M. Sastre, J. Szymanowski, Recovery of zinc(II) from HCl spent pickling solutions by solvent extraction, *Environ. Sci. Technol.*, 35 (2001) 630–635.

- [40] I. Miesiac, J. Szymanowski, Separation of zinc(II) from hydrochloric acid solutions in a double Lewis cell, *Solvent Extr. Ion Exch.*, 22 (2004) 243–265.
- [41] A. Kargari, T. Kaghazchi, M. Soleimani, Role of emulsifier in the extraction of gold (III) ions from aqueous solutions using the emulsion liquid membrane technique, *Desalination*, 162 (2004) 237–247.
- [42] A. Gherrou, H. Kerdjoudj, R. Molinari, E. Drioli, Removal of silver and copper ions from acidic thiourea solutions with a supported liquid membrane containing D2EHPA as carrier, *Sep. Purif. Technol.*, 28 (2002) 235–244.
- [43] R.C. Reid, J.M. Prausnitz, B.E. Poling, *The properties of gases and liquids*, McGraw-Hill, Inc., New York, 1987.
- [44] A.H.P. Skelland, G.G. Ramsay, Minimum agitator speeds for complete liquid-liquid dispersion, *Ind. Eng. Chem. Res.*, 26 (1987) 77–81.
- [45] R.A. Bartsch, E.G. Jeon, W. Walkowiak, W. Apostoluk, Effect of solvent in competitive alkali metal cation transport across bulk liquid membranes by a lipophilic lariat ether carboxylic acid carrier, *J. Membr. Sci.*, 159 (1999) 123–131.